

Heralded quantum steering over a high-loss channel

Morgan M. Weston,¹ Sergei Slussarenko,¹ Helen M. Chrzanowski,^{1,2} Sabine Wollmann,¹ Lynden K. Shalm,³ Varun B. Verma,³ Michael S. Allman,³ Sae Woo Nam,³ and Geoff J. Pryde¹

¹*Centre for Quantum Dynamics and Centre for Quantum Computation and Communication Technology, Griffith University, Brisbane, Queensland 4111, Australia*

²*Clarendon Laboratory, University of Oxford, Parks Road, Oxford OX1 3PU, UK*

³*National Institute of Standards and Technology, 325 Broadway, Boulder, Colorado 80305, USA*

(Dated: March 25, 2022)

Entanglement is the key resource for many long-range quantum information tasks, including secure communication, networking quantum computers, and remote processing of quantum information [1–4]. As the characteristic trait of quantum mechanics [5], it is also important for testing quantum physics over long distances or in different reference frames [6, 7]. Robust verification of remote shared entanglement is highly sought after, as it permits these fundamental tests and protocols such as device-independent quantum key distribution [8, 9]. However, performing these tasks rigorously over long distances is presently technologically intractable because optical fibre, atmospheric or diffraction losses open up a “detection loophole” [10]. Here we design and experimentally demonstrate an event-ready scheme which verifies entanglement in the presence of at least 14.8 ± 0.1 dB of added loss, equivalent to approximately 80 km of telecommunication fibre. Our protocol relies on entanglement swapping to herald the presence of a photon after the lossy channel, enabling event-ready implementation of quantum steering [11] with the detection loophole closed. This result overcomes the key barrier in device-independent communication under realistic high-loss scenarios, and in the realization of a quantum repeater.

A reliable method to send quantum information—from Alice to Bob, say—over long distances is to teleport it, using entanglement shared by the two remote parties [1]. This entanglement resource could alternatively be used for generating secure correlated randomness between Alice and Bob, or efficiently completing shared computational tasks, or testing nonlocality and quantum mechanics in new regimes such as when the parties are in different relativistic reference frames. All of these applications reach their potential only when entanglement is distributed over a long distance. Photons are excellent carriers of the quantum information, being a quantum version of the optical encodings used in existing long-distance classical telephony and data networking. However, in the quantum regime, attenuation (photon loss) is very destructive, because the noise added by this process corrupts the entanglement. Thus, the maximum length of a quantum communication channel is restricted by propagation loss and environmental contamination.

Importantly, the most secure quantum communication approaches—device-independent protocols [8, 12]—and the most robust tests of nonlocality and quantum mechanics require verification of entanglement with strin-

gent conditions on the amount of tolerable loss. For example, complete entanglement verification, through a violation of a Bell inequality, has recently been performed with the three main loopholes [13] closed simultaneously [14–16]. Though these results represent a significant advance, practical limitations remain in exploiting these tests in a realistic long-distance scenario. Inevitable losses through any fibre or free-space channel open the detection loophole for standard photonic implementations, forbidding a robust test even when the post-selected measurement correlations are strong enough to violate a Bell inequality.

Here, in order to overcome the effect of loss in quantum channel, we adopt an *event-ready* approach [17]. The key idea is to record an additional, heralding signal that indicates whether the quantum state under investigation was successfully shared between Alice and Bob—that is, whether the particles are ready to be used in the verification protocol. By conditioning the validity of the protocol trial on this heralding signal, failed distribution events are excluded beforehand from being used in the test. We use entanglement swapping [18–20] to realize an event-ready scheme, allowing us to perform entanglement verification, loophole-free, over lossy quantum communication channels. Our approach also represents a central element of a more complex quantum repeater architecture, which may be used to overcome loss in very large networks.

We use an alternative test of nonlocality, quantum steering (also called EPR-steering). Steering is an asymmetric protocol where one party, Bob, trusts quantum mechanics to describe his own measurements, while no assumptions are made about Alice, the other, untrusted, party [11, 21]. The test may be satisfied by using entanglement to steer the state of a distant quantum system by local measurements on its counterpart. The nonlocal correlations verified by steering are a strict superset of those witnessed by Bell inequalities, but a strict subset of those established by entanglement witnesses. Therefore, a loophole-free test of quantum steering both guarantees shared entanglement and may be configured, with certain conditions, to implement one-sided device-independent QKD [12]. In quantum steering, Alice’s task is to convince Bob that she can influence his quantum measurement outcome for any choice of measurement setting that Bob provides to her. The formal steering protocol is shown in figure 1a: (1) Alice prepares a photon pair and

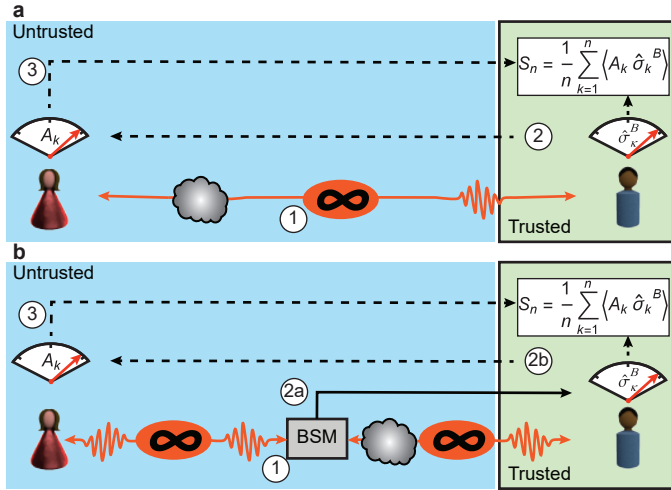


Fig. 1. Conceptual representation of the quantum steering protocols. The blue background denotes untrusted channel components that belong to Alice and the green background denotes the trusted side, Bob. **a**, Conventional steering: (1) Alice prepares a pair of photons and sends one of them to Bob; (2) Bob announces his measurement setting, k , from a predetermined set of n observables; (3) Bob records his measurement outcome $\hat{\sigma}_k^B$ and Alice declares her result A_k ; steps 1 to 3 are iterated to obtain the steering parameter S_n . **b**, Heralded quantum steering protocol. Bob uses a classical signal from a successful BSM measurement (2a) to herald the presence of Alice's photon after the lossy channel, ignoring all the trials when the BSM was not successful.

sends one of the photons to Bob; (2) Bob announces to Alice his choice of measurement settings (labeled k) from a predetermined set of n observables; (3) Bob records his measurement outcome and Alice's declares her result A_k . Steps 1–3 are iterated to obtain the average correlations between Alice's and Bob's result, known as the steering parameter [21]

$$S_n \equiv \frac{1}{n} \sum_{k=1}^n \langle A_k \hat{\sigma}_k^B \rangle, \quad (1)$$

where Bob's k -th measurement setting corresponds to the Pauli observable $\hat{\sigma}_k^B$ for $k \in \{1, \dots, n\}$. We make no assumptions about what Alice is doing, and thus represent her results as $A_k \in \{-1, 1\}$. If S_n is larger than a certain bound C_n [21], then Alice has successfully demonstrated quantum steering. Correct timing of these events is necessary to close the locality loophole [22] and Bob must have truly random measurement choices in order to close the freedom of choice loophole. However, the focus of this work is on transmission loss. A dishonest Alice—or an eavesdropper controlling Alice's apparatus—may attempt to use the fair sampling assumption (i.e. an open detection loophole) to cheat, by hiding incompatible measurement results [10]. She may mimic perfect correlations of a maximally entangled state, and Bob has no

way to determine whether a lack of measurement outcome announcement by Alice is due to genuine qubit loss or cheating. To prevent cheating, Bob requires Alice to announce her measurement result at least a certain fraction ε of trials, which we call Alice's heralding efficiency. When the entanglement verification is performed over long distances, the additional loss in Alice's channel will inevitably reduce the heralding efficiency below an acceptable value required for loophole-free entanglement verification.

The generalised steering bounds, which take into account Alice's heralding efficiency, allow detection-loophole-free quantum steering in presence of arbitrarily high loss in the untrusted quantum channel. However, guaranteed success for very high channel loss relies on the use of perfect pure entangled states and an infinite number of measurement settings, which is unrealistic in real-world scenarios. Though the loss-tolerant protocol has been demonstrated over 1 km of optical fibre [23], real life applications will have much higher losses, imperfect states, and finite number of pre-selected measurement settings n , so eventually the protocol will fail.

Implementing an event-ready entanglement verification scheme allows us to herald the presence of the qubit in Alice's arm, increasing her effective heralding efficiency. In principle, this improved heralding could be realised in one of several ways, broadly including quantum-non-demolition-style measurements such as entanglement swapping [18–20] and distillation techniques such as noiseless linear amplification [24, 25]. For the levels of loss considered here, we favour entanglement swapping, owing to its comparatively low resource overhead and high success rates. If entanglement swapping is performed with spontaneous parametric downconversion (SPDC) sources, as here, the squeezing parameter of those sources must be chosen carefully to control the effect of multiphoton events (see Methods).

The effective increase in heralding efficiency obtained with the entanglement swapping step allows us to avoid the detection loophole without assuming the honesty of Alice. Crucially, if the protocol is run in a fully time-ordered mode, as illustrated in Extended Data Figure 1, Alice is forced to announce over a classical channel when the teleportation has been successful, and thus declare which subset of measurement runs should be used to verify the entanglement, before Bob announces his measurement settings. This prevents her exploiting the non-determinism of the swapping operation to introduce a loophole—announcing a false outcome of the entanglement swapping measurement gains her no advantage. Bob can then proceed with the steering verification protocol.

We performed our experiment using two polarization-entangled photon pairs generated by separate high-heralding-efficiency sources [26], S_1 and S_2 (see figure 2 and Methods). The photon pairs were prepared in $|\Psi^-\rangle = (|HV\rangle - |VH\rangle)/\sqrt{2}$, where $|H\rangle$ and $|V\rangle$ denote horizontal and vertical polarizations respectively. The

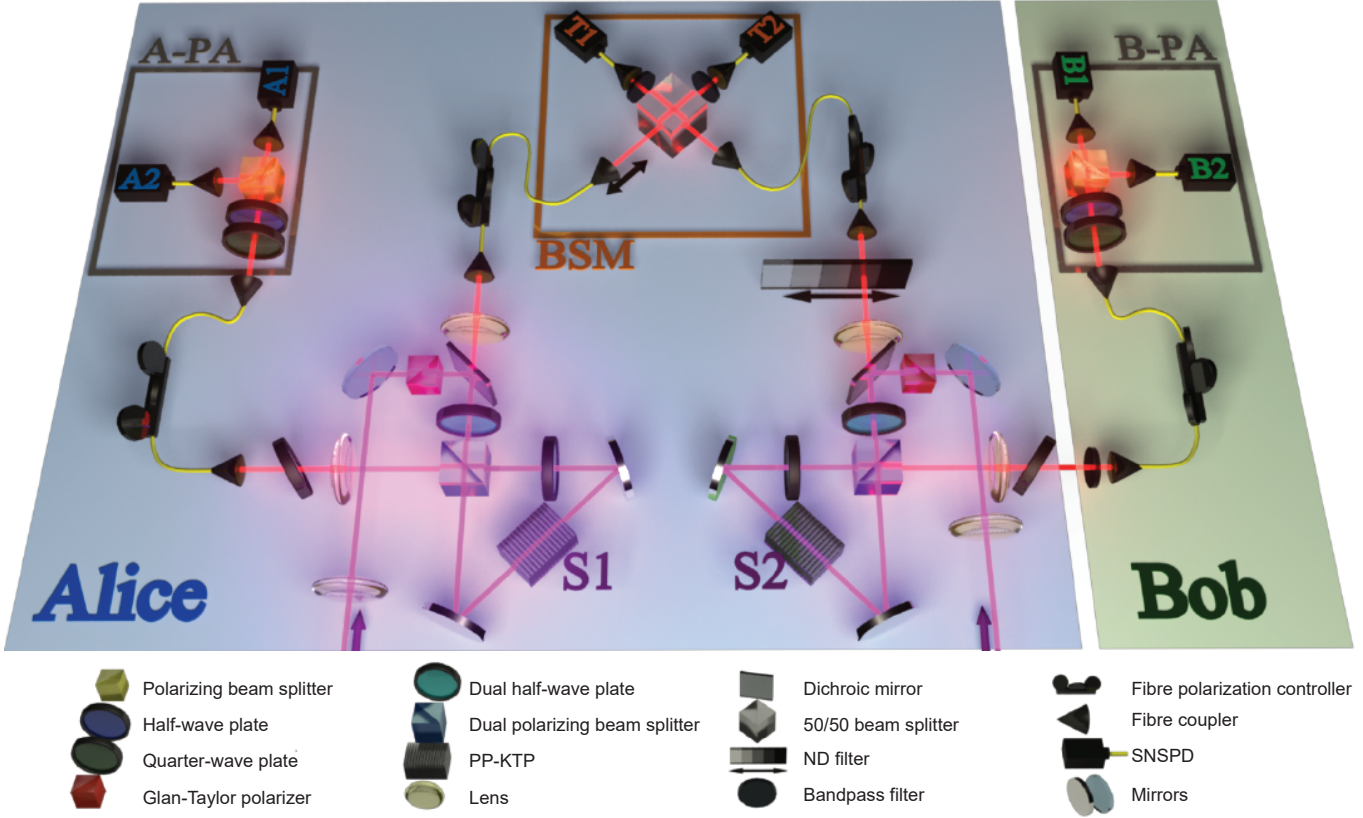


Fig. 2. Experimental setup. Two group-velocity-matched sources S_1 and S_2 are pumped by a mode-locked femtosecond Ti:Sapphire laser to generate two polarization-entangled photon pairs at 1570 nm, in the $|\Psi^-\rangle$ state (see Methods for details). Blue and green backgrounds outline the untrusted and trusted sides respectively. (All untrusted elements are grouped with Alice, even if they are not in her “lab” in practice.) A-PA and B-PA are the polarization analysis (tomography) stages of Alice and Bob, and BSM is the Bell state measurement gate, comprised of a non-polarizing 50/50 beam splitter. A variable neutral density (ND) filter is used in the Alice’s arm of S_2 to introduce the channel loss, \mathcal{L} . 8 nm bandpass filters (BP) were placed in the path of the photon going to B-PA and after BS increasing the singlet state fidelity, while maintaining Alice’s high heralding efficiency. For the conventional steering measurement, Alice’s arm of S_2 was directly connected to the A-PA stage through the fiber, bypassing the BSM gate and S_1 .

signal photon from source S_2 was sent to Bob for polarization analysis (B-PA) measurement, while remaining photon from the same pair was sent through a variable-loss channel towards Alice. In the first experiment, only source S_2 was used, and Alice’s channel contained no added loss. Alice directly received her photon from S_2 into her polarization analyzer (A-PA)—no entanglement swapping was employed. We performed the steering protocol with $n = 6$ measurement settings [23] and a heralding efficiency for Alice of $\varepsilon = 0.4395 \pm 0.0003$ in the protocol, and observed detection-loophole-free quantum steering with a steering parameter of $S_6 = 0.960 \pm 0.008$, violating the C_n bound by 18 standard deviations.

In the second experiment, a variable channel loss \mathcal{L} was added between the two parties by using gradient neutral density (ND) filter (see figure 2). Using only source S_2 , we measured the steering parameter S_6 and Alice’s effective heralding efficiency for various levels of added channel loss. The results are shown in figure 3c.

With the addition of even 7.7 ± 0.1 dB of channel loss, the heralding efficiency dropped below the $C_\infty(\varepsilon)$ bound, forbidding secure quantum steering even in the limiting theoretical case of infinite measurement settings.

In the third experiment, we added source S_1 and the entanglement swapping step to herald Alice’s photon. Since S_1 does not have unit heralding efficiency, the entanglement swapping does not produce deterministic arrival of a photon at Alice polarization measurement. However, it increases this probability to a level compatible with demonstrating detection-loophole-free steering: her conditional heralding efficiency was recovered to $\varepsilon \sim 0.45$ (Fig. 3c).

The entanglement swapping works as follows. The photon Alice receives from S_2 and one photon from S_1 are inputs to a Bell state measurement (BSM) gate, where they are interfered non-classically. (The remaining photon from S_1 was sent to Alice’s polarization analyzer.) A coincidence detection signal from the two BSM detec-

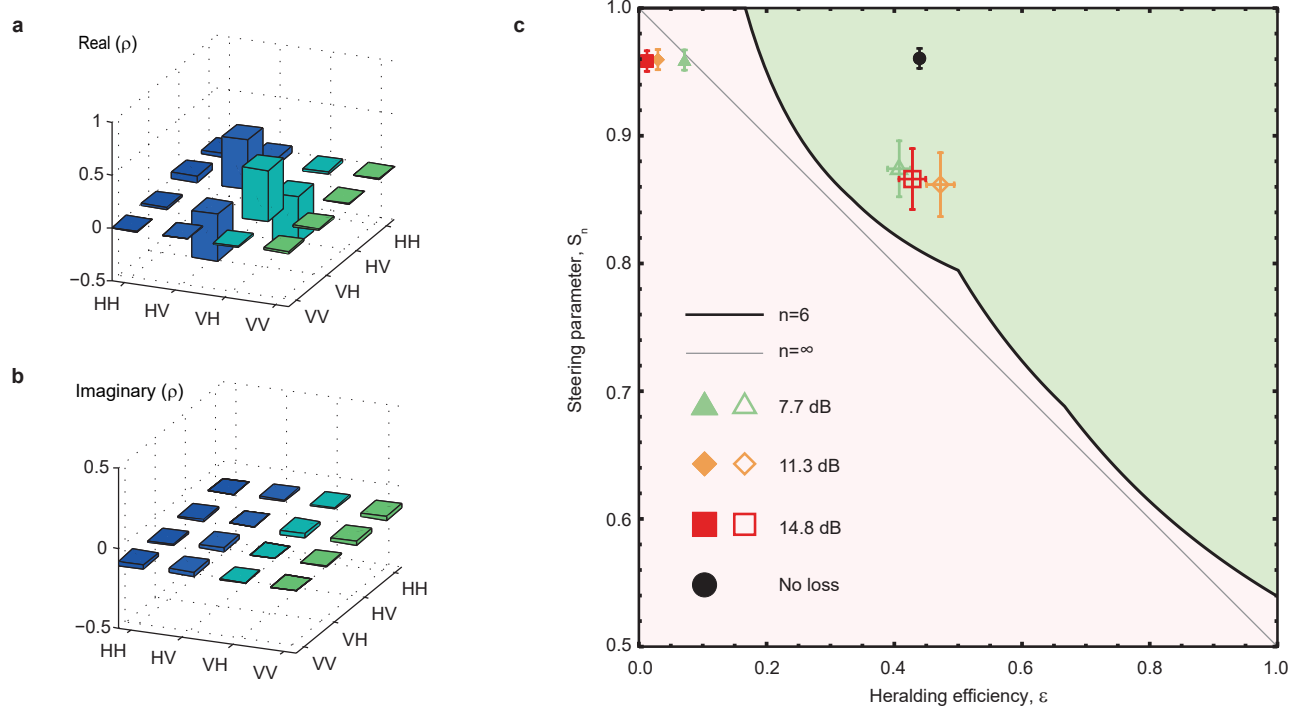


Fig. 3. Experimental results. **a**, Real and **b**, Imaginary part of the reconstructed density matrix ρ of the entanglement-swapped two-photon state with no additional loss applied to the quantum channel. The state fidelity with $|\Psi^-\rangle$ is $\mathcal{F} = (91 \pm 3)\%$. **c**, Quantum steering measurement results for different amount of channel loss. Solid thick and thin lines are, respectively, the $C_6(\varepsilon)$ and $C_\infty(\varepsilon)$ steering bounds from [23], and green and red backgrounds highlight the parameter regions where detection loophole-free steering with $n = 6$ measurements is achievable or not, respectively. The black solid circle marks the steering parameter measured with the conventional quantum steering protocol in the absence of loss and without entanglement swapping. Green triangles, yellow diamonds and red squares correspond to the steering parameters measured in presence of 7.7 ± 0.1 , 11.3 ± 0.1 and 14.8 ± 0.1 dB of added channel loss respectively. Filled markers correspond to steering parameters measured with the conventional steering protocol. Empty markers correspond to steering parameters measured with the heralded quantum steering, each calculated from at least 500 four-fold coincidence counts. Steering parameters 0.874 ± 0.022 , 0.862 ± 0.022 and 0.866 ± 0.024 , measured with the heralded steering protocol are at least 2.2 standard deviations above the $C_6(\varepsilon)$ steering bound for corresponding values of heralding efficiency 0.41 ± 0.02 , 0.47 ± 0.02 and 0.43 ± 0.02 (in order of increasing loss).

tors labels a successful projection onto the $|\Psi^-\rangle$ state, heralding a successful swapping operation. Alice's effective heralding efficiency at A-PA is now defined as the probability of detecting a four-photon coincidence from A-PA, B-PA and the triggers at the BSM, given that a three-photon coincidence was detected from B-PA and the two-photon trigger at the BSM. High-visibility Hong-Ou-Mandel interference is required in order to perform the swapping operation with high fidelity. This was possible to achieve, while maintaining high entangled state fidelity and high heralding efficiency, thanks to our high-performance sources [26] and high-efficiency, low-noise superconducting nanowire single photon detectors [27] (see Methods for details). The final shared state ρ , with no added loss, was determined using quantum state tomography [28] and is shown in figure 3a,b. It had a singlet Bell state fidelity $\mathcal{F} = \langle \Psi^- | \hat{\rho} | \Psi^- \rangle = (91 \pm 3)\%$ which is comparable with the best previously reported in entanglement swapping [29].

With the heralded steering protocol, we observed successful violation of the $C_6(\varepsilon)$ bound by at least 2.2 standard deviations (see Methods for details on uncertainties estimation) while adding up to 14.8 ± 0.1 dB of channel loss, equivalent to 74–82 km of telecom optical fibre, assuming fibre loss of 0.18–0.2 dB/km. It is worth noting that Alice's total channel loss, including the loss due to optical components in the BSM gate but excluding the detector efficiency, amounts to 20.0 ± 0.1 dB, which is equivalent to at least 100 km of telecom fibre.

As seen from figure 3b, we have not observed any degradation in the measured steering parameter or heralding efficiency while increasing the amount of channel loss. This result suggests that the protocol is not limited to the demonstrated 14.8 ± 0.1 dB of added (20.0 \pm 0.1 dB total) loss, and that achieving heralded quantum steering with higher values of loss is possible. As the main breakthrough of our work is closing the detection loophole over a high-loss channel, we did not im-

plement randomized choice of measurement settings and time order of detection events in any of the steering protocol experiments.

Our heralded quantum steering protocol is the first demonstration of detection-loophole-free entanglement verification over a high loss channel. The ability to keep the quantum steering detection loophole closed with total losses of at least 20 ± 0.1 dB, and potentially higher, opens many new possibilities for security in long range transmission through optical fibre, free space, or between earth and satellite. With additional assumptions, it has been previously been shown how to make a measurement-device-independent version of the steering protocol [30] and how to turn quantum steering into a one-sided device-independent quantum key distribution scheme [12]. The result we achieved is a considerable step towards the implementation of secure quantum communication, and represents a single step quantum relay, a crucial component for future quantum repeaters.

I. METHODS

A. Photon sources and characterization

The heralded quantum steering protocol relies on pure and indistinguishable entangled states. Conventional spontaneous parametric downconversion (SPDC) sources require narrowband (FWHM < 2 nm) filters to erase the spectral distinguishability. These filters significantly decrease the heralding efficiency, making a detection-loophole-free steering inequality violation impossible. To circumvent this obstacle, we developed a new type of SPDC photon source [26]. Our sources work at the group velocity matching (GVM) condition to generate frequency uncorrelated photon pairs, removing the necessity of harsh spectral filtering.

We used two such polarization-entangled photon pair sources in the Sagnac interferometer configuration (\mathcal{S}_1 and \mathcal{S}_2 in figure 2), pumped by a mode-locked Ti:Sapphire laser with 81 MHz repetition rate, 785 nm wavelength and 5.35 nm FWHM bandwidth. In each source, SPDC from a nonlinear periodically poled KTP crystal produced photon pairs with 1570 nm wavelength and ≈ 15 nm FWHM bandwidth. The Sagnac configuration provided polarization entanglement, while the pump and crystal parameters were selected to remove frequency correlations. The focusing and collection Gaussian beam modes were optimized to increase the heralding efficiency of the source, according to ref. [26]. Together with high efficiency superconducting nanowire single photon detectors (SNSPD) [27] we achieved heralding efficiencies of 0.47 ± 0.02 for each of our sources, while maintaining the necessary high fidelity of entanglement swapping.

The entangled states produced by \mathcal{S}_1 and \mathcal{S}_2 were characterized, one at a time, via polarization state tomography. For each state we used either A-PA or B-PA for one of the photon measurements. To measure the other pho-

ton in a pair, an additional polarization measurement stage inserted in the BSM gate part of the setup (not shown in figure 2). The fidelity with the maximally-entangled singlet Bell state, measured in this way, was $\mathcal{F} = (97.2 \pm 0.3)\%$ for \mathcal{S}_1 , where both photons were filtered with 8 nm bandpass filters, and $\mathcal{F} = (98.2 \pm 0.3)\%$ for \mathcal{S}_2 , where the spectral filtering was applied only to the photon passing through the BSM part of the apparatus. Although the source needs very little spectral filtering in principle, this moderate filtering was employed to overcome reductions in the fidelity caused by wavelength-dependent effects introduced by some optical components.

We measured Hong-Ou-Mandel interference visibility in the BSM gate in order to characterize the indistinguishability of the photons from \mathcal{S}_1 and \mathcal{S}_2 . One photon from each maximally entangled pair was sent into BSM, while the remaining photons of each pair were sent into A-PA and B-PA gates and projected into the $\{|H\rangle, |V\rangle\}$ basis. We used 8 nm bandpass filters at the output of the BSM stage and on the heralding photon of the \mathcal{S}_2 photon pair. No polarization optics were used inside the BSM gate. We observed visibilities of $(90 \pm 3)\%$ for $|V\rangle$ polarized photons and $(99 \pm 4)\%$ for $|H\rangle$ polarized photons. We attribute the lower visibility value to the residual polarization distinguishability of interfering photons, arising from the non-symmetric (47 : 53) splitting ratio of our BS for vertical polarization and, more significantly, from the lack of spectral flatness of optical coatings of optical components over the wide frequency band of our photons.

B. Channel loss

Alice's added channel loss, \mathcal{L} , was implemented by using two variable neutral density (ND) filters, whose transmission was characterized separately using a 1570 nm diode laser. 8 nm BP filters introduced an additional 3.5 ± 0.1 dB of loss, and the loss due to optical components and fiber coupling of the BSM gate was measured to be 1.7 ± 0.1 dB. Together with $\mathcal{L} = 14.8 \pm 0.1$ dB of maximum added loss, the highest total loss applied to the channel was 20 ± 0.1 dB, excluding the non-unit quantum efficiency of the SNSPDs.

C. High order SPDC pair generation

The pumping powers $P(S_n)$ of our sources were kept below 100 mW in order to keep negligible the impact of high-order pair production on the independent HOM interference and state quality [26, 31]. In the presence of added loss, the fractional contribution of high order terms from \mathcal{S}_1 increases. However, the probability of generating a photon pair from each source is comparable with the probability of generating two photon pairs from \mathcal{S}_2 . The latter events produce false heralding coincidences,

significantly decreasing Alice's heralding efficiency (see Extended Data Figure 2). Efficient heralding of entanglement swapping requires that the number of photons from one side (e.g. source \mathcal{S}_2) is significantly lower than the number of photons from the other side (source \mathcal{S}_1). With the increased channel loss, this condition is satisfied automatically even for equal raw brightness of \mathcal{S}_1 and \mathcal{S}_2 . Nevertheless, careful selection of appropriate pump powers for these sources is still required. We found that as the loss was increased, $P(\mathcal{S}_1)$ had to be decreased in order to keep the swapped state quality high, and $P(\mathcal{S}_2)$ had to be matched accordingly to maintain the heralding efficiency. The pump powers chosen for different levels of added loss are shown in Extended Data Table 1.

Though the protocol can theoretically hold for arbitrarily high loss, increasing the loss significantly reduces the count rates. Increasing loss will eventually result in unrealistic count times, and in spurious coincidence rates caused by dark and background counts becoming comparable to real coincident photon detections.

D. Experimental uncertainties

The measurement uncertainties for the quantum steering parameters comprise heralding efficiency uncertainty and steering parameter uncertainty, denoted by horizontal and vertical error bars respectively in figure 3b. The latter takes into account both systematic measurement error and Poissonian photon counting noise. The systematic error contribution occurs due to the imperfections in optical components of Bob's measurement apparatus, which could result in an overestimate of the steering parameter. We used the systematic error estimation procedure developed in ref. [23]. This procedure assumes a perfect entangled state, and attributes any deviation from $S_n = 1$ to the imperfection of Bob's measurement apparatus. Such an approach overestimates the steering parameter systematic uncertainty, when applied to our experimental data, where $S_n < 1$ is known to arise predominantly from imperfect entangled states and imperfect entanglement swapping. The uncertainties in state parameters derived from quantum state tomography were calculated through standard error propagation techniques applied to a distribution of reconstructed density matrices arising from a Monte Carlo calculation which samples from Poissonian distributions of photon counts.

[1] M. Nielsen and I. Chuang, *Quantum Computation and Quantum Information*, Cambridge Series on Information and the Natural Sciences (Cambridge University Press, 2000).

[2] R. Horodecki, P. Horodecki, M. Horodecki, and K. Horodecki, "Quantum entanglement," *Rev. Mod. Phys.* **81**, 865 (2009).

[3] T. Ralph and G. Pryde, "Optical quantum computation," *Prog. Optics* **54**, 209 (2009).

[4] G. Y. Xiang, B. L. Higgins, D. W. Berry, H. M. Wiseman, and G. J. Pryde, "Entanglement-enhanced measurement of a completely unknown optical phase," *Nat. Photon.* **5**, 43 (2011).

[5] E. Schrödinger, "Discussion of Probability Relations between Separated Systems," *Math. Proc. Cambridge* **31**, 555 (1935).

[6] D. Rideout, T. Jennewein, G. Amelino-Camelia, T. F. Demarie, B. L. Higgins, A. Kempf, A. Kent, R. Laflamme, X. Ma, R. B. Mann, E. Martin-Martinez, N. C. Menicucci, J. Moffat, C. Simon, R. Sorkin, L. Smolin, and D. R. Terno, "Fundamental quantum optics experiments conceivable with satellites reaching relativistic distances and velocities," *Class. Quantum Grav.* **29**, 224011 (2012).

[7] P. M. Alsing and I. Fuentes, "Observer-dependent entanglement," *Class. Quantum Grav.* **29**, 224001 (2012).

[8] A. Acín, N. Gisin, and L. Masanes, "From Bell's Theorem to Secure Quantum Key Distribution," *Phys. Rev. Lett.* **97**, 120405 (2006).

[9] L. C. Comandar, M. Lucamarini, B. Frhlich, J. F. Dynes, A. W. Sharpe, S. W.-B. Tam, Z. L. Yuan, R. V. Penty, and A. J. Shields, "Quantum key distribution without detector vulnerabilities using optically seeded lasers," *Nat. Photon.* **10**, 312 (2016).

[10] P. M. Pearle, "Hidden-Variable Example Based upon Data Rejection," *Phys. Rev. D* **2**, 1418 (1970).

[11] H. M. Wiseman, S. J. Jones, and A. C. Doherty, "Steering, Entanglement, Nonlocality, and the Einstein-Podolsky-Rosen Paradox," *Phys. Rev. Lett.* **98**, 140402 (2007).

[12] C. Branciard, E. G. Cavalcanti, S. P. Walborn, V. Scarani, and H. M. Wiseman, "One-sided device-independent quantum key distribution: Security, feasibility, and the connection with steering," *Phys. Rev. A* **85**, 010301 (2012).

[13] J.-Å. Larsson, "Loopholes in Bell inequality tests of local realism," *J. Phys. A* **47**, 424003 (2014).

[14] L. K. Shalm, E. Meyer-Scott, B. G. Christensen, P. Bierhorst, M. A. Wayne, M. J. Stevens, T. Gerrits, S. Glancy, D. R. Hamel, M. S. Allman, K. J. Coakley, S. D. Dyer, C. Hodge, A. E. Lita, V. B. Verma, C. Lambrocco, E. Tortorici, A. L. Migdall, Y. Zhang, D. R. Kumor, W. H. Farr, F. Marsili, M. D. Shaw, J. A. Stern, C. Abellán, W. Amaya, V. Pruneri, T. Jennewein, M. W. Mitchell, P. G. Kwiat, J. C. Bienfang, R. P. Mirin, E. Knill, and S. W. Nam, "Strong Loophole-Free Test of Local Realism," *Phys. Rev. Lett.* **115**, 250402 (2015).

[15] M. Giustina, M. A. M. Versteegh, S. Wengerowsky, J. Handsteiner, A. Hochrainer, K. Phelan, F. Steinlechner, J. Kofler, J.-A. Larsson, C. Abellán, W. Amaya, V. Pruneri, M. W. Mitchell, J. Beyer, T. Gerrits, A. E. Lita, L. K. Shalm, S. W. Nam, T. Scheidl, R. Ursin,

B. Wittmann, and A. Zeilinger, "Significant-Loophole-Free Test of Bell's Theorem with Entangled Photons," *Phys. Rev. Lett.* **115**, 250401 (2015).

[16] B. Hensen, H. Bernien, A. E. Dreau, A. Reiserer, N. Kalb, M. S. Blok, J. Ruitenberg, R. F. L. Vermeulen, R. N. Schouten, C. Abellán, W. Amaya, V. Pruneri, M. W. Mitchell, M. Markham, D. J. Twitchen, D. Elkouss, S. Wehner, T. H. Taminiau, and R. Hanson, "Loophole-free Bell inequality violation using electron spins separated by 1.3 kilometres," *Nature* **526**, 682 (2015).

[17] M. Żukowski, A. Zeilinger, M. A. Horne, and A. K. Ekert, "Event-ready-detectors" Bell experiment via entanglement swapping," *Phys. Rev. Lett.* **71**, 4287 (1993).

[18] J.-W. Pan, D. Bouwmeester, H. Weinfurter, and A. Zeilinger, "Experimental Entanglement Swapping: Entangling Photons That Never Interacted," *Phys. Rev. Lett.* **80**, 3891 (1998).

[19] R. Kaltenbaek, R. Prevedel, M. Aspelmeyer, and A. Zeilinger, "High-fidelity entanglement swapping with fully independent sources," *Phys. Rev. A* **79**, 040302 (2009).

[20] R.-B. Jin, M. Takeoka, U. Takagi, R. Shimizu, and M. Sasaki, "Highly efficient entanglement swapping and teleportation at telecom wavelength," *Sci. Rep.* **5**, 9333 (2015).

[21] D. J. Saunders, S. J. Jones, H. M. Wiseman, and G. J. Pryde, "Experimental EPR-steering using Bell-local states," *Nature Phys.* **6**, 845 (2010).

[22] B. Wittmann, S. Ramelow, F. Steinlechner, N. K. Langford, N. Brunner, H. M. Wiseman, R. Ursin, and A. Zeilinger, "Loophole-free Einstein-Podolsky-Rosen experiment via quantum steering," *New J. Phys.* **14**, 053030 (2012).

[23] A. J. Bennet, D. A. Evans, D. J. Saunders, C. Branciard, E. G. Cavalcanti, H. M. Wiseman, and G. J. Pryde, "Arbitrarily Loss-Tolerant Einstein-Podolsky-Rosen Steering Allowing a Demonstration over 1 km of Optical Fiber with No Detection Loophole," *Phys. Rev. X* **2**, 031003 (2012).

[24] S. Kocsis, G. Y. Xiang, T. C. Ralph, and G. J. Pryde, "Heralded noiseless amplification of a photon polarization qubit," *Nature Phys.* **9**, 23 (2013).

[25] A. E. Ulanov, I. A. Fedorov, A. A. Pushkina, Y. V. Kurochkin, T. C. Ralph, and A. I. Lvovsky, "Undoing the effect of loss on quantum entanglement," *Nat. Photon.* **9**, 764 (2015).

[26] M. M. Weston, H. M. Chrzanowski, S. Wollmann, A. Boston, J. Ho, L. K. Shalm, V. B. Verma, M. S. Allman, S. W. Nam, R. B. Patel, S. Slussarenko, and G. J. Pryde, "Efficient and pure femtosecond-pulse-length source of polarization-entangled photons," *Opt. Express* **24**, 10869 (2016).

[27] F. Marsili, V. B. Verma, J. A. Stern, S. Harrington, A. E. Lita, T. Gerrits, I. Vayshenker, B. Baek, M. D. Shaw, R. P. Mirin, and S. W. Nam, "Detecting single infrared photons with 93% system efficiency," *Nat. Photon.* **7**, 210 (2013).

[28] A. G. White, A. Gilchrist, G. J. Pryde, J. L. O'Brien, M. J. Bremner, and N. K. Langford, "Measuring two-qubit gates," *J. Opt. Soc. Am. B* **24**, 172 (2007).

[29] Q.-L. Wu, N. Namekata, and S. Inoue, "High-fidelity entanglement swapping at telecommunication wavelengths," *J. Phys. B* **46**, 235503 (2013).

[30] S. Kocsis, M. J. W. Hall, A. J. Bennet, D. J. Saunders, and G. J. Pryde, "Experimental measurement-device-independent verification of quantum steering," *Nat. Commun.* **6**, 5886 (2015).

[31] J. Fulconis, O. Alibart, W. J. Wadsworth, and J. G. Rarity, "Quantum interference with photon pairs using two micro-structured fibres," *New J. Phys.* **9**, 276 (2007).

Acknowledgements

Part of this work is supported by ARC grant DP140100648 and part of this work is supported by ARC grant CE110001027. Authors thank Joseph Ho for help with SNSPDs.

Author contributions

GJP conceived the idea, HMC and GJP designed the experiment. MMW, SS and HMC constructed and carried out the experiment with help and supervision from GJP. MMW and SS analyzed the data. SW assisted in early stages of development. LKS, VBV, MSA and SWN developed high efficiency SNSPDs. All authors discussed the results and contributed to the manuscript.